

Effect of surfactant concentration on saturated flow boiling in vertical narrow annular channels

G. Hetsroni *, M. Gurevich, A. Mosyak, R. Rozenblit

Department of Mechanical Engineering, Technion – Israel Institute of Technology, Haifa 32000, Israel

Received 12 July 2006; received in revised form 14 November 2006

Abstract

Saturated flow boiling of environmentally acceptable nonionic surfactant solutions of Alkyl (8–16) was compared to that of pure water. The concentration of surfactant solutions was in the range of 100–1000 ppm. The liquid flowed in an annular gap of 2.5 and 4.4 mm between two vertical tubes. The heat was transferred from the inner heated tube to two-phase flow in the range of mass flux from 5 to 18 kg/m² s and heat flux from 40 to 200 kW/m². Boiling curves of water were found to be heat flux and channel gap size dependent but essentially mass flux independent. An addition of surfactant to the water produced a large number of bubbles of small diameter, which, at high heat fluxes, tend to cover the entire heater surface with a vapor blanket. It was found that the heat transfer increased at low values of relative surfactant concentration C/C_0 , reaches a maximum close to the value of $C/C_0 = 1$ (where $C_0 = 300$ ppm is the critical micelle concentration) and decreased with further increase in the amount of additive. The dependence of the maximal values of the relative heat transfer enhancement, obtained at the value of relative concentration of $C/C_0 = 1$, on the boiling number Bo may be presented as single curve for both gap sizes and the whole range of considered concentrations.

© 2007 Elsevier Ltd. All rights reserved.

Keywords: Flow boiling; Surfactant solution; Heat transfer; Narrow space; Annular channel

1. Introduction

In boiling heat transfer, it is usually desirable to transfer the largest possible heat flux with the smallest possible temperature difference between the heating surface and the boiling liquid. A number of experimental studies have been conducted on flow boiling water in small size channels. Wambsganss et al. (1993) have investigated flow boiling of refrigerant R 113 in a small circular tube of $D = 2.92$ mm. The mass flux m and heat flux q were varied in the following range: $m = 50$ – 300 kg/m² s, $q = 8.8$ – 90.8 kW/m². Their results showed that the flow boiling heat transfer coefficient was a strong function of the applied heat flux (i.e. it increases with increasing heat flux keeping all other parameters fixed) and was only weakly dependent on mass flux and vapor quality. Tran et al. (1996) have performed nucleate boiling heat transfer studies using a horizontal, small rectangular channel (height of 4.06 mm, width of 1.70 mm) which had a hydraulic diameter of

* Corresponding author. Tel.: +972 4 8292058; fax: +972 4 8238101.
E-mail address: hetsroni@techunix.technion.ac.il (G. Hetsroni).

2.40 mm. The test fluid was refrigerant R 12. The following ranges of mass fluxes and heat fluxes were covered in their study $m = 50\text{--}400 \text{ kg/m}^2 \text{ s}$, $q = 4\text{--}34 \text{ kW/m}^2$. Their experimental results supported the earlier results of Wambsganss et al. (1993) in that nucleate boiling was the dominant heat transfer mechanism. The nucleate boiling heat transfer coefficient was found to be strongly dependent on heat flux but almost independent of mass flux. Bao et al. (2000) studied the flow boiling heat transfer characteristics of refrigerants R 11 and HCFC1 123 in horizontal, small diameter tube of $D = 1.95 \text{ mm}$. Experiments were performed in the range of mass fluxes $m = 50\text{--}1800 \text{ kg/m}^2 \text{ s}$ and heat fluxes $q = 5\text{--}200 \text{ kW/m}^2$. Their results are similar to those reported by other researches, in that the heat transfer coefficient is a strong function of the heat flux, but almost independent of mass flux. Yu et al. (2002) studied boiling heat transfer of water in a small horizontal tube of 2.98 mm inner diameter. Experiments were performed at system pressure of 200 kPa, mass fluxes $m = 50\text{--}200 \text{ kg/m}^2 \text{ s}$, heat fluxes $q = 5\text{--}200 \text{ kW/m}^2$. The inlet fluid temperature was from ambient to 353 K. It was shown that mass flux and inlet temperature effects were minimal.

Pool boiling heat transfer in a confined narrow space was investigated by Fujita et al. (1988) for saturated water at atmospheric pressure. The heat transfer coefficient increased up to a certain value with a decrease in the gap size at moderate heat flux, while degradation occurred for a further decrease of the gap size over the whole heat flux range. Reducing the channel dimension was found to produce a negative effect on the boiling heat transfer in the tubes of 2.39–3.69 mm (Kew and Cornwell, 1997). Though they mentioned that the heat transfer data could be correlated using the confinement number, $N_c = (\sigma/g\Delta\rho)^{0.5}/D_h$ where $(\sigma/g\Delta\rho)^{0.5}$ is the Laplace constant, σ is the surface tension, $\Delta\rho$ is the difference between fluid and vapor density, g is the acceleration due to gravity, no correlation was given. It should be stressed that the dependence of N_c on the acceleration due to gravity g seemed having little relevance outside of pool boiling.

A number of investigators reported the opposite effect. Kureta et al. (1998) investigated flow boiling of water in tubes of 2.0–6.0 mm at mass fluxes $m = 100\text{--}10,170 \text{ kg/m}^2 \text{ s}$ with an inlet subcooling of 70–90 K under atmospheric pressure condition. They reported that measured heat transfer coefficients were less, compared to that of a tube with a diameter which is much larger than the Laplace constant, since the heat transfer due to turbulent mixing agitated by vapor bubbles was suppressed. Kaminaga et al. (2000) conducted an experiment on boiling heat transfer in small tubes of 1.45 and 2.8 mm with water under natural circulation condition. They observed that when the tube diameter was less than the Laplace constant the heat transfer coefficient was much higher than the conventional pool boiling. Sumith et al. (2003) studied the characteristics of flow boiling heat transfer in a vertical tube of 1.45 mm diameter, which is less than the Laplace constant. Heat transfer coefficients were measured in the range of mass fluxes from 23.4 to 152.7 $\text{kg/m}^2 \text{ s}$, heat fluxes from 10 to 715 kW/m^2 . Large heat transfer enhancement was observed. The dominant flow pattern in the tube was a slug-annular or an annular flow, and then liquid film evaporation was found to dominate the heat transfer. Jacobi and Thome (2002) demonstrate that transient evaporation of the thin liquid films surrounding elongated bubbles is the dominant heat transfer mechanism in microchannels, not nucleate boiling. Thome et al. (2004) cited the following classification of the transition from macroscale to microscale based on the hydraulic diameter: microchannels (1–100 μm), mesochannels (100 μm –1 mm), macrochannels (1–6 mm) and conventional channels (>6 mm). They noted that such transition criteria do not reflect the influence of channel size on the physical heat transfer mechanism. Therefore the authors suggest that the best threshold criterion is that the bubble growth is confined by the channel, such the bubbles grow in length rather than in diameter.

Forced convective boiling of steam-water in annular channels was studied recently by Barbosa et al. (2002, 2003), and Situ et al. (2004a,b). At low qualities (of a few percent), there was a dominance of nucleate boiling. At high qualities nucleate boiling was partly or totally suppressed and forced convection may become the dominant mechanism. The heat transfer coefficient might remain constant, decrease or increase depending on the contribution of these two mechanisms during forced convection boiling. Lie and Lin (2005) investigated how the channel size affects the saturated flow boiling heat transfer of refrigerant R 134a in a horizontal narrow annular duct. The gap of the duct was fixed at 1.0 and 2.0 mm. It was found that the saturated flow boiling heat transfer coefficient increases with a decrease in gap size. Besides, raising the imposed heat flux can cause a significant increase in the boiling heat transfer coefficient.

It was shown by Tzan and Yang (1990), Wu et al. (1995), Yang and Maa (1983, 2001), Wasekar and Manglik (1999, 2000, 2002), Yang et al. (2002), Hetsroni et al. (2001, 2002, 2004a), and Zhang and Manglik (2005) that addition of a small amount of surfactant significantly decreased the bubble size. Under these conditions

the heat transfer coefficient increases in saturated boiling of surfactants compared with that in pure water. Heat exchangers with small channels are prevalent in many industries such as electronic, transport, and chemical processing. The surface tension force is important and might affect flow patterns and heat transfer in such channels.

Hetsroni et al. (2004a) studied boiling heat transfer in an annular space between two vertical tubes with gap size of 4.4 mm. The working fluids were water and a solution of Alkyl (8–16) Glycoside, having negligible environmental impact, for the single surfactant concentration of 300 ppm. The heat was transferred from the inner heated tube to the outer one. The authors have considered the development of the flow boiling pattern along the heater direction. They noted that the average heat transfer of the surfactant solution may be up to four times higher than that of pure water in the saturated flow boiling region and that boiling curves of surfactant solution demonstrated unusual behavior, i.e. at low heat flux the temperature of the heated wall decreased with an increase in heat flux.

The present study is an extension of the above mentioned research aimed at finding an effect of the surfactant concentration and gap size on the boiling heat transfer. No studies were found on this phenomenon for flow boiling of surfactant solutions in annular channels. Specially, saturated flow boiling at low values of mass fluxes was studied because it facilitated understanding of the process in compact heat exchangers.

2. Experimental apparatus and procedure

2.1. Experimental apparatus

Fig. 1 shows a schematic view of the experimental apparatus. The experimental system (Fig. 1a) consists of several sub-systems that include the degassing section, flow development section, test section, data acquisition system, high-speed imaging system. The working fluid is deionized and degassed water. The degassing procedure was followed before beginning and during the experiments. It consists of fluid boiling before the experiments for 2 h at a pressure of 1 bar and then boiling over the period of the experiments. The heat input for degassing was supplied by a heater (1). The water temperature in the degassing section was measured by a thermometer (3). Whilst the experiments were carried out boiling in the entrance tank (2) took place and the fluid at saturation temperature moved to thermostat (4) that controls the inlet temperature to the development section. Pump (5) delivered the fluid to the inlet manifold (7). The flow rate of the working fluid was controlled by a valve and measured by a rotameter (6). The development section consisted of the outer stainless steel tube (8) and the inner stainless steel rod (9). One end of the rod was connected to the electrical contact the second was soldered to the inner stainless steel tube (10).

Two test sections with different gap sizes of 2.5 and 4.4 mm were used. The test section (Fig. 1b) consisted of central stainless steel tube (10) with an outer diameter $d_1 = 3.2$ mm or $d_2 = 4.0$ mm and a wall thickness of 0.3 mm and glass tube (11) with inner diameter of $D_1 = 12$ and $D_2 = 9.0$ mm, respectively. The central tube was heated by passing DC electrical current from a low voltage, high current power supply. The temperature on the heated wall of the test section was measured by a radiation equilibrium thermocouple (12) (Hetsroni et al., 2004a) that could be moved along the tube (10) to any desired position in the heated tube. The annulus was formed between the heated tube (10) and unheated glass tube (11). The location of the thermocouple junction is determined by the scale (14), marked on a cover of thermocouple wires. The temperature on the outer wall of the glass tube was measured by thermocouples to estimate the heat losses.

The local temperatures of the fluid, which passed through the test section, were measured by means of the moving thermocouple (13), inserted into the annulus. The steam-water mixture generated in the annular channel of the test section was directed through the outlet manifold (15) and tube (16) to the tank (2). Such method of liquid temperature measurement allows determining of the local temperature of the liquid along the heated tube more precisely, compared with the study of Hetsroni et al. (2004a) where liquid temperature was determined by an interpolation of readings of separate thermocouples placed in the side pockets. The pressure readings were taken from pressure taps (P) at the inlet and outlet of the test section. Experiments were performed at atmospheric pressure. Heat transfer data were taken as the heat flux was increased, as well as with heat flux being decreased step by step. Direct observation of the flow was carried out by using a high-speed video recording system (17) with recording rate up to 10,000 frames per second, mounted on the tripod.

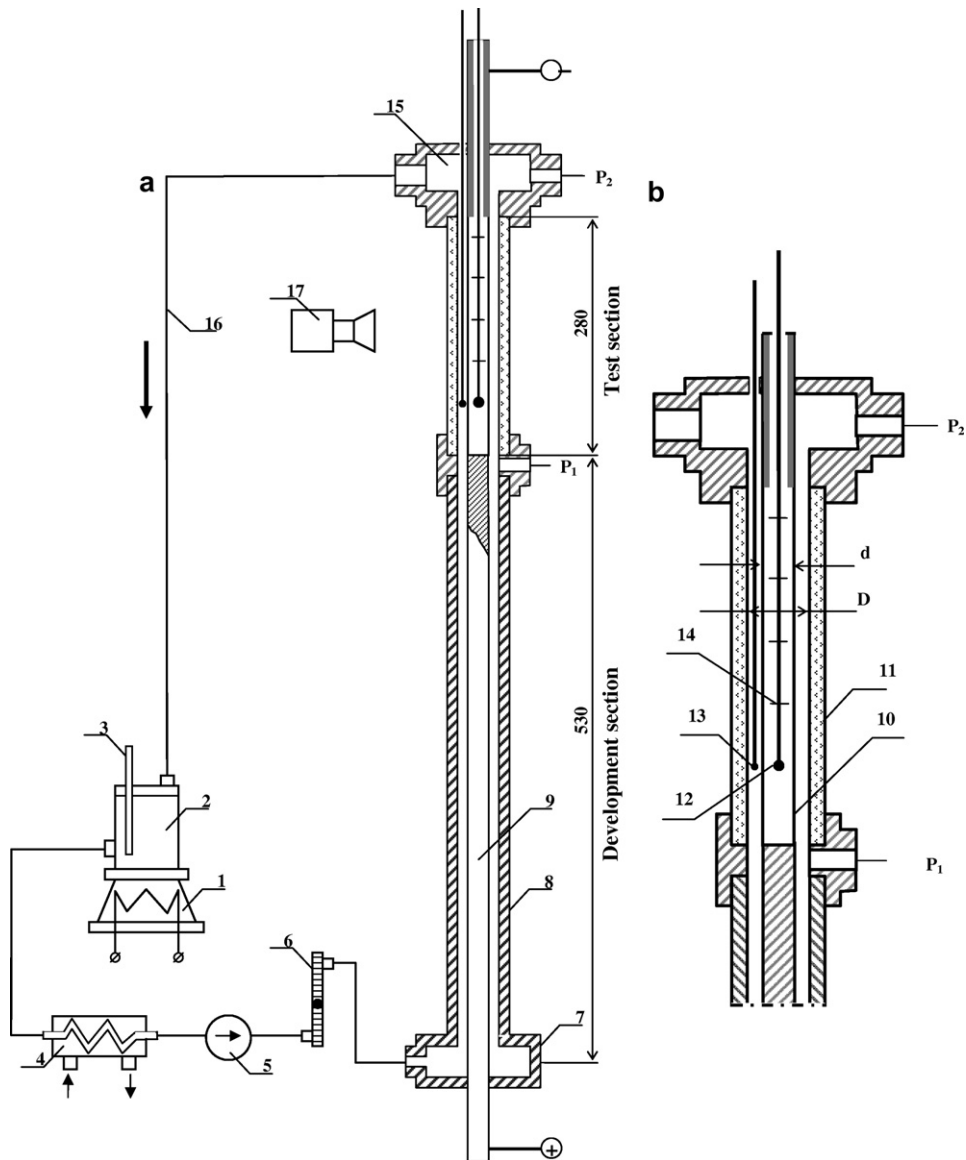


Fig. 1. Experimental apparatus. (a) Schematic diagram of experimental facility: 1 – heater, 2 – entrance tank, 3 – thermometer, 4 – thermostat, 5 – pump, 6 – rotameter, 7 – inlet manifold, 8 – outer stainless steel tube, 9 – rod, 15 – outlet manifold, 16 – tube, 17 – video system and (b) test section: 10 – inner heated stainless steel tube, 11 – outer glass tube, 12 – thermocouple for measurements of outer surface of the heated tube, 13 – thermocouple for the measurements of the liquid which passed through the annulus of the test section, 14 – scale.

2.2. Properties of surfactant solutions

We used Alkyl (8–16) Glycoside nonionic surfactant solution of molecular weight 390 g/mol. The measurements of surface tension were carried out for different concentrations of surfactant solutions over a range of temperature from 300 K to 368 K. In Fig. 2 the equilibrium surface tension, σ , is plotted vs. the concentration of the surfactant solution at different temperatures. An increase in surfactant concentration up to $C = 300$ ppm (parts per million weight) leads to significant decrease in surface tension. In the range $300 \leq C \leq 1200$ ppm the surface tension was almost independent of concentration. In all cases an increase in liquid temperature leads to a decrease in surface tension. In the present study, the range of concentration

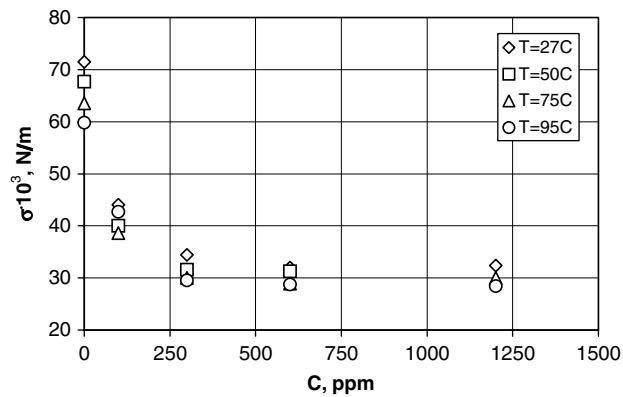


Fig. 2. Surface tension of Alkyl (8–16) solution vs. concentration at different temperatures.

was $C = 100\text{--}1000$ ppm. The solutions were prepared by dissolving the surfactant (52% active substance and 48% water) in deionized water, with gentle stirring over a period of a one-day.

2.3. Error analysis

Electrical power was determined with an accuracy of 0.5%. The surface heat flux was calculated by measuring the power delivered to the heated inner surface and by determination of heat losses. The temperature of the heated surface and of the working fluid was measured by 0.3 mm type-T thermocouples. The thermocouples and the data acquisition system were calibrated at the steam point and ambient water temperature, and yield values within 0.3 K at these two conditions. The rotameter was calibrated at its operating temperatures with an accuracy of 1%. The estimated accuracy in the calculation of the saturation temperature is 0.1 K. The error associated with the measurement of the distances between the thermocouple locations is 0.5 mm. In order to calculate the deviations associated with the measurement of various quantities, readings were taken for a few sample runs every 2 min over a period of 20 min. The uncertainty analysis was performed according to the ASME Policy on Reporting Uncertainties in Experimental Measurements and Results. The results of the uncertainty analysis are given in Table 1, where the bias limit is an estimate of the magnitude of the fixed constant error. The precision limit is an estimate of the lack of repeatability caused by random errors and unsteadiness. The uncertainty in the heat transfer coefficient with 95% confidence interval is between 9% and 16%. The uncertainty is higher at the higher values of heat transfer coefficient due to the small temperature difference between the wall and the fluid.

2.4. Experimental runs

First the liquid flow rate and the liquid temperature at the inlet ($T_0 = 303 \pm 1$ K) of the setup were established. The electrical power of the heater was then gradually increased. For each value of heat flux, when steady state was attained, the wall temperature was measured at various distances along the heater. Simultaneously the location of a zone with the liquid saturation temperature was determined by the thermocouple moved along the heated tube in the annular space. It was assumed that steady state was reached when the

Table 1
Uncertainty of the measurements

Item	Designation	Bias limit B	Precision limit P (%)
Heat flux	q	1 kW/m ²	2.0
Wall temperature	T_w	0.3 K	1.0
Bulk temperature	T_f	0.5 K	2.0
Saturation temperature	T_s	0.1 K	0.2
Mass flow rate	m	0.04 kg/m ² s	2.0
Location along the heater	x	0.5 mm	5

thermocouple reading at the given position was steady. Experiments were conducted under conditions at which the CHF regime did not occur. Thus, at given value of fluid inlet temperature and flow rate the maximum operating heat flux did not exceed the value at which the heating surface temperature would rise suddenly. Afterwards, electrical power was gradually decreased and measurements were conducted under conditions of decreasing heat flux.

A fresh sample of surfactant solution was used after three runs. This precaution was taken to minimize changes in solution properties, which might have occurred at high temperature due to evaporation over a long period of time. No visible deposits formed under test conditions, based on observations in the test runs and after draining the test section.

The heat flux was determined as

$$q_w = (N - N_{\text{loss}}) / \pi d_1 L \quad (1)$$

where N is the electrical power, N_{loss} are the heat losses, d_1 is the outer diameter of the heated tube, L is the heated length.

The heat transfer coefficient, α , in the saturated boiling region was calculated by the relationship:

$$\alpha = q_w / (T_w - T_s) \quad (2)$$

where q_w is the heat flux, T_w , and T_s is the local wall temperature and saturation temperature, respectively.

More accurate prediction of heat transfer coefficients requires the correct thermal boundary conditions. To simplify the full three-dimensional conjugate analysis the following thermal boundary condition is used: circumferentially constant wall temperature and axially constant heat flux. Lee et al. (2005) concluded that such thermal boundary condition is the most appropriate for simplified analyses, when a full conjugate analysis is not affordable. This thermal boundary condition is common in engineering problems such as electric resistance heating, counter-flow heat exchangers, etc.

That is why the value of heat transfer coefficient α according to Eq. (2) is a good enough approximation of a true local heat transfer value.

3. Results

The saturation condition under thermodynamic equilibrium is reached at some distance x_0 from the entrance of the test section. This point is identified as the onset of saturated flow boiling, or OSB. Heat transfer beyond OSB the saturation flow boiling region is the main focus of the present study. In this region the complex interactions between the liquid film close to the heater and the bubbles in the bulk flow take place. In this case the bulk fluid temperature $T_f = T_s$. From flow visualization the experimental evidence of OSB is characterized by the end of condensation. The bubbles start to fill the whole cross-section of the annular channel. It was shown by Hetsroni et al. (2004a) that for both water and surfactant solution the onset of saturation boiling occurs at the same distance from the inlet.

Flow visualization showed that for water, bubble action was seen to be extremely chaotic, with extensive coalescence during the rise. An addition of small amount of surfactant makes the behavior of the boiling quite different from that of pure water. Bubbles formed in surfactant solutions were much smaller than those of water. It is known that reduced surface tension results in a decrease of the energy required to initiate bubble growth and thus in an increase in the quantity of bubbles and a decrease in their diameter.

We consider next boiling curves obtained in the saturation boiling region. It was noted that an addition of small amount of surfactant drastically changed the boiling curve, thus first of all we consider the effect of surfactant additive on the flow boiling in the annular channels with different gap sizes at the lowest concentration of 100 ppm (1 g of the surfactant in 10,000 g of water) in the surfactant solution and after that we will estimate the effect of an increase in the level of the surfactant concentration.

3.1. Effect of mass flux

Fig. 3 shows boiling curves of water and surfactant solution of concentration $C = 100$ ppm at mass flux of 5.0 and 8.3 kg/m² s in the annular channel with gap size ($d_2 - d_1$) of $\delta = 4.4$ mm. The saturated boiling data of

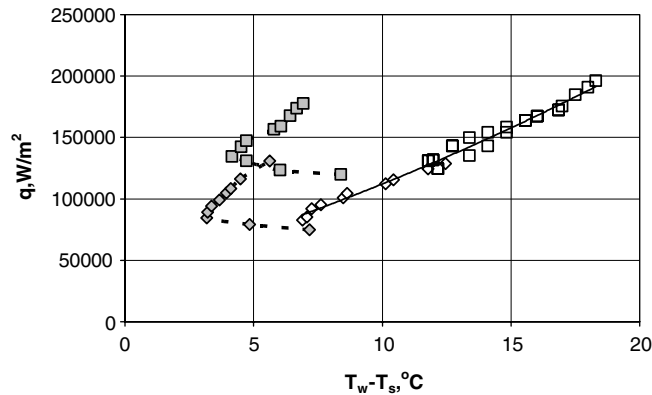


Fig. 3. Boiling curves of water and surfactant solution of $C = 100$ ppm concentration at mass flux of 5.0 and 8.3 $\text{kg/m}^2 \text{s}$ in the annular channel with gap size of $\delta = 4.4$ mm. Symbols: \diamond – mass flux of 5.0 $\text{kg/m}^2 \text{s}$; \square – mass flux of 8.3 $\text{kg/m}^2 \text{s}$; the clear water (not filled symbols); the surfactant solution (grey symbols).

water in this channel were compared to the measurements conducted in narrow space by Fujita et al. (1988). In that study, experiments on heat transfer characteristics in pool boiling were performed in a confined space bounded by a rectangular heating surface and an opposed unheated plate. We compared our data in the saturated boiling zone to those presented by Fujita et al. (1988) for gap size of 5 mm, closed side periphery, and the length of the heating surface of 120 mm. Their gap size is close to the hydraulic radius of the test section, $r_h = 4.4$ mm, used in the present study. The comparison of results obtained in our annular channel with data of Fujita et al. (1988) showed that the agreement was acceptable. One may conclude that under conditions of saturated water flow boiling the mass flux did not affect the behavior of boiling curve. This conclusion agrees with results discussed by Barbosa et al. (2002), Hetsroni et al. (2004a), and Lie and Lin (2005).

Boiling curve for surfactant solution of 100 ppm concentration demonstrates unusual behavior, i.e. at low heat flux the temperature of the heated wall decreases with an increase in the heat flux. At high values of heat flux the temperature of the heated wall increases with an increase in heat flux. Each point in Fig. 3 and in the following figures represents an average value obtained from these measurements for increasing heat flux and remaining four runs for decreasing heat flux. We did not observe any signs of hysteresis.

Analogous results were obtained at the channel with gap size of $\delta = 2.5$ mm. Fig. 4 shows boiling curves of water and surfactant solution of $C = 100$ ppm concentration at mass flux $m = 8.3$ and 18 $\text{kg/m}^2 \text{s}$. Water flow boiling experimental results can also be described by a single curve. Similar results were found previously by Wambsganss et al. (1993), Tran et al. (1996), Bao et al. (2000), Yu et al. (2002), Sumith et al. (2003), and Hetsroni et al. (2004a). From flow visualization of water flow boiling Hetsroni et al. (2004) also concluded that the heat transfer enhancement is due to a heat transfer regime transition from nucleate boiling to thin liquid film evaporation. For surfactant solution of $C = 100$ ppm one can conclude that the boiling curve shifts to higher values of wall superheat with an increase in mass flux.

In narrow channels, bubble sizes can grow to the size of the channel spacing rapidly if the heat flux is high enough. In this regime the dynamics of bubble formation assumes special significance and has to be included as a major parameter that affects the boiling process. Visualization of boiling of surfactant solution showed clusters of small bubbles, which penetrated the thin liquid film near the heated wall. The increase in the mass flux affects mixing of the liquid film agitated by small vapor bubbles. It may be possible to conclude that the agitated liquid film evaporation is important in contributing the flow boiling heat transfer of surfactants in a narrow annular duct.

3.2. Effect of gap channel size

Comparison between results presented in Figs. 3 and 4 for water boiling shows that at low values of heat flux the boiling curves do not differ significantly at heat flux $q < 100 \text{ kW/m}^2$ for $\delta = 4.4$ mm and $\delta = 2.5$ mm.

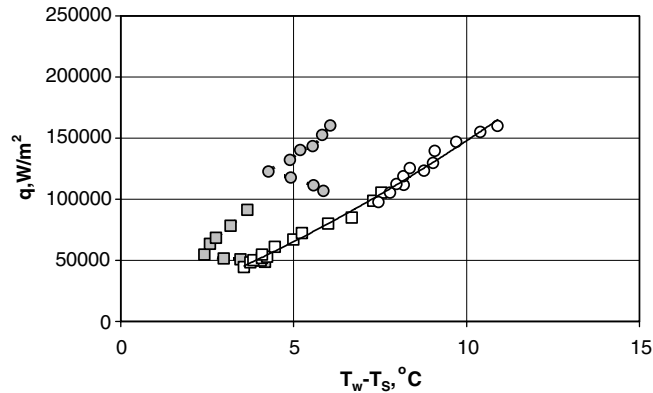


Fig. 4. Boiling curves of water and surfactant solution of $C = 100$ ppm concentration at mass flux $m = 8.3$ and $18 \text{ kg/m}^2 \text{ s}$ in the annular channel with gap size of $\delta = 2.5$ mm. Symbols: \diamond – mass flux of $8.3 \text{ kg/m}^2 \text{ s}$; \circ – mass flux of $18 \text{ kg/m}^2 \text{ s}$; the clear water (not filled symbols); the surfactant solution (grey symbols).

However, at higher values of heat flux, (of about 150 kW/m^2), a decrease in the channel size leads to heat transfer enhancement. These results are in the agreement with those reported by Barbosa et al. (2002, 2003), Situ et al. (2004a,b), and Lie and Lin (2005). The effect of the decrease in the gap size from 4.4 mm to 2.5 mm on the heat transfer in the surfactant solution is examined more carefully in Fig. 5, where boiling curves for water and surfactant are presented at the same mass flow rate $8.3 \text{ kg/m}^2 \text{ s}$. It can be seen that the upper parts of boiling curves for surfactant solution are similar to the water boiling curves, but at lesser temperature differences at the same heat flux, whereas the lower parts of boiling curves are parallel and almost anti-symmetric to the corresponding boiling curve.

A decrease in the channel gap size significantly reduces the maximum heat flux for surfactant solution. It is due to the delay of bubble departure and early dryout of the heated wall in high heat flux region. It should be stressed that the experiments in the present study were carried out in the range of heat fluxes that were much lower than CHF.

3.3. Effect of surfactant concentration

To clarify the effect of an increase in the surfactant concentration on boiling curve we conducted the experiments for surfactant solutions of four concentrations (100, 300, 600 and 1000 ppm) at different mass flow

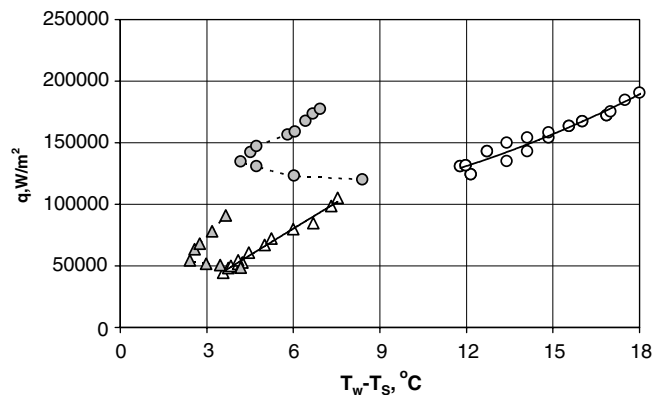


Fig. 5. Boiling curves of water and surfactant solution in the annular channels of the different gap size at the same mass flux $8.3 \text{ kg/m}^2 \text{ s}$: Symbols: \triangle – gap size of 2.5 mm; \circ – gap size of 4.4 mm; the clear water (not filled symbols); the surfactant solution of 100 ppm (grey symbols).

rates and two gap sizes of annular channel. Fig. 6 shows, for example, typical boiling curves for various concentrations in tubes with gap of 4.4 mm (Fig. 6a) and of 2.5 mm (Fig. 6b), at the same mass flow rate of $8.3 \text{ kg/m}^2 \text{ s}$. It can be seen that the effect of concentration on flow boiling of surfactant solution becomes complicated. Boiling curve of 100 ppm solution is sharply shifted to the left at low heat fluxes, reached the minimal value of the temperature difference, corresponding to the maximum of heat transfer coefficient, and then again sharply shifted right crossing other curves at larger concentration for both gaps of the annular channel. Boiling curve of 300 ppm has a maximal shift to the left, consequently provided the maximal enhancing of heat transfer at flow boiling. The shift is less pronounced for the boiling curves in the surfactant solution of 600 and 1000 ppm.

This phenomenon may be considered more carefully (Fig. 7) by presenting these data in a form of the dependence of the relative heat transfer enhancement $h/h_w - 1$ on the relative concentration C/C_0 at some definite value of the boiling number $Bo = q/mh_{LG}$, where h and h_w are the heat transfer coefficients in surfactant solutions and pure water, respectively, C is the concentration of surfactant solution, C_0 is the critical micelle concentration (CMC), h_{LG} is the latent heat of evaporation. The CMC is a significantly important characteristic of surfactants, as it demarcates the transition in both the liquid–vapor and solid–liquid interfacial phenomena. The surface tension of a given surfactant solution reaches the lowest possible value at CMC. It was found by Hetsroni et al., 2004b that $C_0 = 300 \text{ ppm}$ for surfactant solutions used in the present study. Post-CMC, surfactant molecules tend to form bilayers (or other micellar layers) on the solid surface to make it strongly hydrophilic, (Zhang and Manglik, 2005). The curves presented in Fig. 7 have different value of heat transfer enhancement depending on channel gap size, boiling number Bo and relative concentration of the solution. However, they have similar trends with increasing surfactant concentration C/C_0 . Heat transfer increases at low values of C/C_0 , reaches a maximum at $C/C_0 = 1$, further increase in the amount of additive leads to a decrease in the relative heat transfer coefficient.

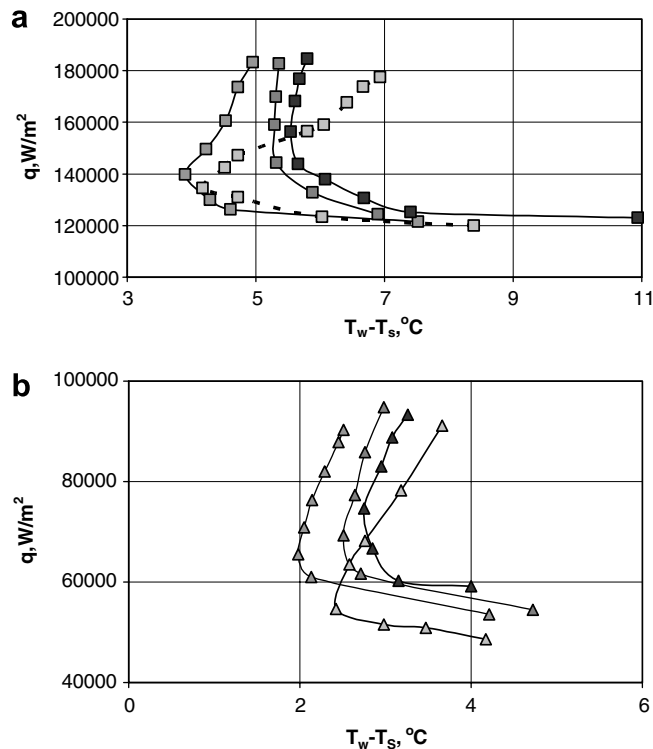


Fig. 6. Boiling curves in the tubes with different gap sizes for various concentrations at the same mass flux of $8.3 \text{ kg/m}^2 \text{ s}$. The gap is: (a) 4.4 mm, (b) 2.5 mm. The grey level is increased according to the increase in the level of the surfactant concentration of 100, 300, 600 and 1000 ppm respectively.

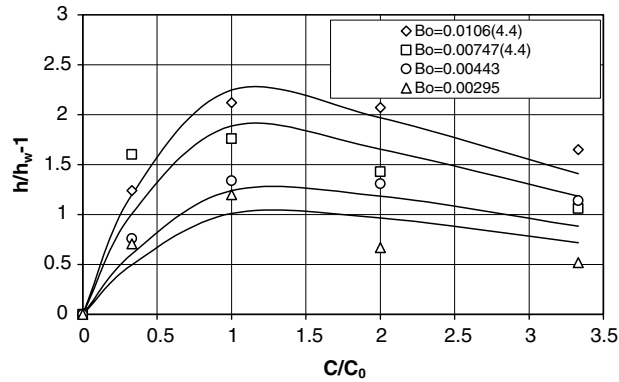


Fig. 7. Dependence of the relative heat transfer enhancement $h/h_w - 1$ in the zones of saturate boiling on the relative concentration C/C_0 at some typical values of the boiling number Bo in the tube of both gap sizes. Continuous lines are the computation according to Eq. (3) at the same Bo number.

The opposite tendency was observed relative to the bubble diameter. Fig. 8 presents the images recorded by high-speed video of a zone of saturated boiling on the tube for various concentrations of the surfactant. We can see that the bubble diameter has the minimum at the CMC of 300 ppm. It is precisely this surfactant concentration that the heat transfer coefficient has the maximum. These pictures also show that only bubbles of clear water are confined slightly by the gap size in the zone of saturated boiling, whereas the mean bubble diameter in the surfactant solution is well lesser than the gap size. This fact suggests that, according to the Thome et al. (2004) model, the evaporation is not dominant mechanism of heat transfer in the conditions of this experiment.

The enhancement of heat transfer at saturated flow boiling of Alkyl (8–16) Glycoside solution in the annular channel of gap size 2.2 and 4.4 mm may be estimated with an average uncertainty of 12% by the following correlation:

$$\bar{h} = 1 + \frac{55.15\bar{d}\bar{C}Bo^{0.5}}{1 + 1.08\bar{d}(1 + \bar{C}^2)} \quad (3)$$

where $\bar{h} = h/h_w$ is the heat transfer enhancement, $\bar{d} = (D - d)/d$ is the relative diameter, Bo is the boiling number and $\bar{C} = C/C_0$ is the relative surfactant concentration. According to this correlation the relative heat transfer enhancement ($\bar{h} - 1$) is proportional to the relative surfactant concentration \bar{C} at low surfactant concentrations and it is inversely proportional to \bar{C} at high concentrations $\bar{C}^2 \gg 1$. Thus, the enhancement of heat transfer might be explained mainly by the behavior of the surface tension in this range of concentrations. However, it was shown by Wasekar and Manglik (2000, 2002), Hetsroni et al. (2001, 2002, 2004), and Zhang and Manglik (2005) that besides the effects of concentration of surfactant and its chemistry (ionic nature and

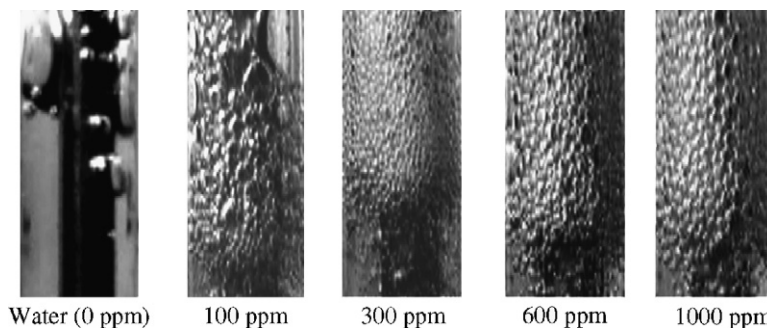


Fig. 8. Images of a zone of saturated boiling on the tube for various concentrations of the surfactant (the gap size is 2.5 mm).

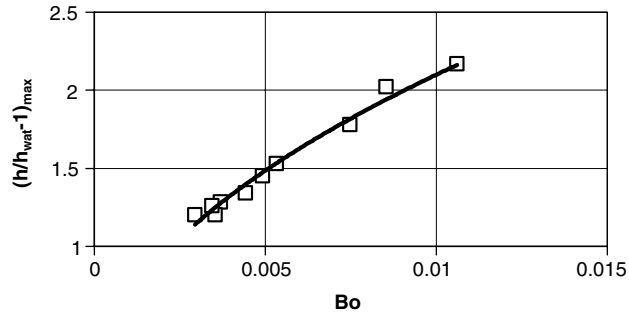


Fig. 9. Dependence of the maximal values of the relative heat transfer enhancement $(\bar{h} - 1)_{\max}$ obtained at $C/C_0 = 1$ on the boiling number Bo .

molecular weight), dynamic surface tension, surface wetting, Marangoni convection, surfactant adsorption and desorption and foaming must be considered to have a significant influence.

Fig. 9 shows the dependence of the maximal values of the relative heat transfer enhancement $(\bar{h} - 1)_{\max}$ obtained at $C/C_0 = 1$ on the boiling number Bo . It can be seen that this dependence may be presented as single curve for both gap sizes and whole range of considered concentrations:

$$(\bar{h} - 1)_{\max} = 21Bo^{0.5} \quad (4)$$

4. Conclusions

Under conditions of saturated water flow boiling the mass flux did not affect the behavior of the boiling curve. Addition of small amount of surfactant to water changes the boiling curve drastically. At the same value of heat flux the temperature difference $(T_w - T_s)$ for boiling of surfactant solution is significantly smaller than that for pure water. Boiling curve for surfactant solution demonstrates unusual behavior, i.e. at low heat fluxes the temperature of the heated wall decreases with an increase in the heat flux. For surfactant solutions the boiling curves shift to higher values of wall superheat with an increase in mass flux. This effect was observed in the whole range of solution concentrations. An increase in mass flux affects mixing of the liquid film agitated by small vapor bubbles.

A decrease in the channel gap size significantly reduces the maximum heat flux for the surfactant solution. It is due to the delay of bubble departure and early dryout of the heated wall in high heat flux region.

The curves of the relative heat transfer enhancement $h/h_w - 1$ depends on the relative concentration C/C_0 of the surfactant solution, dimensionless gap size and the boiling number Bo , however they have similar trends with increasing surfactant concentration C/C_0 . Heat transfer increases at low values of C/C_0 , reaches a maximum close to the value of $C/C_0 = 1$, further increase in the amount of additive leads to a decrease in the relative heat transfer coefficient.

The dependence of the maximal values of the relative heat transfer enhancement $(\bar{h} - 1)_{\max}$ obtained at the value of relative concentration of $C/C_0 = 1$ on the boiling number Bo may be presented as single curve for the both gap sizes and whole range of considered concentrations.

Acknowledgements

A. Mosyak and R Rozenblit were supported by a joint grant from the Center for Absorption in Science of the Ministry of Immigrant Absorption and the Committee for Planning and Budgeting of the Council for Higher Education under the framework of the KAMEA PROGRAM.

References

- Bao, Z.Y., Fletcher, D.F., Haynes, B.S., 2000. Flow boiling heat transfer of Freon R11 and HCFC123 in narrow passages. *Int. J. Heat Mass Transfer* 43, 3347–3358.

- Barbosa Jr., J.R., Hewitt, G.F., Richardson, S.M., 2002. Forced convective boiling of steam-water in a vertical annulus at high qualities. *Exp. Therm. Fluid Sci.* 26, 65–75.
- Barbosa Jr., J.R., Hewitt, G.F., Richardson, S.M., 2003. High-speed visualization of nucleate boiling in a vertical annular flow. *Int. J. Heat Mass Transfer* 46, 5153–5160.
- Fujita, Y., Ohta, H., Uchida, S., Nishikawa, K., 1988. Nucleate boiling heat transfer and critical heat flux in narrow space between rectangular surfaces. *Int. J. Heat Mass Transfer* 31, 229–239.
- Hetsroni, G., Zakin, J.L., Lin, Z., Mosyak, A., Pancallo, E.A., Rozenblit, R., 2001. The effect of surfactants on bubble growth, wall thermal patterns and heat transfer in pool boiling. *Int. J. Heat Mass Transfer* 44, 485–497.
- Hetsroni, G., Gurevich, M., Mosyak, A., Rozenblit, R., Yarin, L.P., 2002. Subcooled boiling of surfactant solutions. *Int. J. Multiphase Flow* 28, 347–361.
- Hetsroni, G., Zakin, J.L., Gurevich, M., Mosyak, A., Pogrebnyak, E., Rozenblit, R., 2004a. Saturated flow boiling heat transfer of environmentally acceptable surfactants. *Int. J. Multiphase Flow* 30, 717–734.
- Hetsroni, G., Gurevich, M., Mosyak, A., Rozenblit, R., Segal, Z., 2004b. Boiling enhancement with environmentally acceptable surfactants. *Int. J. Heat Fluid Flow* 25, 841–848.
- Jacobi, A.M., Thome, J.R., 2002. Heat transfer model for evaporation of elongated bubble flows in microchannels. *J. Heat Transfer* 124, 1131–1136.
- Kaminaga, F., Chowdhury, F., Baduge, S., Matsumura, K., 2000. In: *Proc. Boiling 2000: Phenom. Emerging Applicat.* pp. 272–288.
- Kew, P.A., Cornwell, K., 1997. Correlations for the prediction of boiling heat transfer in small diameter channels. *Appl. Therm. Eng.* 17, 705–715.
- Kureta, M., Kobayashi, T., Mishina, K., Nishihara, H., 1998. Pressure drop and heat transfer for flow boiling of water in a small diameter tubes. *JSME Int. J., Series B* 41, 871–879.
- Lee, P.S., Garimella, S.V., Liu, D., 2005. Investigation of heat transfer in rectangular micro-channels. *Int. J. Heat Mass Transfer* 48, 1688–1704.
- Lie, Y.M., Lin, T.F., 2005. Saturated flow boiling heat transfer and associated bubble characteristics of R-134a in a narrow annular duct. *Int. J. Heat Mass Transfer* 48, 5602–5615.
- Situ, R., Mi, Y., Ishii, M., Mori, M., 2004a. Photographic study of bubble behaviors in forced convection subcooled boiling. *Int. J. Heat Mass Transfer* 47, 3659–3667.
- Situ, R., Hibiki, T., Sun, X., Mi, Y., Ishii, M., 2004b. Flow structure of subcooled boiling in an internally heated annulus. *Int. J. Heat Mass Transfer* 47, 5351–5364.
- Sumith, B., Kaminaga, F., Matsumura, K., 2003. Saturated flow boiling of water in a vertical small diameter tube. *Exp. Therm. Fluid Sci.* 27, 789–801.
- Thome, J.R., Dupont, V., Jacobi, A.M., 2004. Heat transfer model for evaporation in microchannels. Part I: presentation of model. *Int. J. Heat Mass Transfer* 47, 3375–3385.
- Tran, T.N., Wambsganss, M.W., France, D.M., 1996. Small circular and rectangular channel boiling with two refrigerants. *Int. J. Multiphase Flow* 22, 485–498.
- Tzan, Y.L., Yang, Y.M., 1990. Experimental study of surfactant effects on pool boiling heat transfer. *J. Heat Transfer* 112, 207–212.
- Wambsganss, M.W., France, D.M., Jendrzeczyk, J.A., Tran, T.N., 1993. Boiling heat transfer in a horizontal small diameter tube. *J. Heat Transfer* 115, 963–972.
- Wasekar, V.M., Manglik, R.M., 1999. A review of enhanced heat transfer in nucleate pool boiling of aqueous surfactant and polymeric solutions. *J. Enhanc. Heat Transfer* 6, 135–150.
- Wasekar, V.M., Manglik, R.M., 2000. Pool boiling heat transfer in aqueous solutions of an anionic surfactant. *J. Heat Transfer, Trans. ASME* 122, 708–715.
- Wasekar, V.M., Manglik, R.M., 2002. The influence of additive molecular weight and ionic nature on the pool boiling performance of aqueous surfactant solutions. *Int. J. Heat Mass Transfer* 45, 483–493.
- Wu, W.T., Yang, Y.M., Maa, J.R., 1995. Enhancement of nucleate boiling heat transfer and depression of surface tension by surfactant additives. *J. Heat Transfer* 117, 526–529.
- Yang, Y.M., Maa, J.R., 1983. Pool boiling of dilute surfactant solutions. *J. Heat Transfer* 105, 190–192.
- Yang, Y.M., Maa, J.R., 2001. On the criteria of nucleate pool boiling enhancement by surfactant addition to water. *Trans. IChemE, Part A* 79, 409–415.
- Yang, Y.M., Lin, C.Y., Liu, M.H., Maa, J.R., 2002. Lower limit of the possible nucleate pool boiling enhancement by surfactant addition to water. *J. Enhanc. Heat Transfer* 9, 153–160.
- Yu, W., France, D.M., Wambsganss, M.W., Hull, J.R., 2002. Two-phase pressure drop, boiling heat transfer, and critical heat flux to water in a small-diameter horizontal tube. *Int. J. Multiphase Flow* 28, 927–941.
- Zhang, J., Manglik, R.M., 2005. Additive absorption and interfacial characteristics of nucleate pool boiling in aqueous surfactant solutions. *J. Heat Transfer* 127, 684–691.